High-mass ρ-meson states from $\bar{p}d$-annihilation at rest into $\pi^-\pi^0\pi^0 p_{spectator}$

Crystal Barrel Collaboration

A. Abele [h], J. Adomeit [g], C. Amsler [p], D.S. Armstrong [a,1], C.A. Baker [e], B.M. Barnett [c], C.J. Batty [e], M. Benayoun [m], A. Berdoz [n], K. Beuchert [b], P. Birien [a], S. Bischoff [h], P. Blüm [h], K. Braune [l], J. Brose [k], D.V. Bugg [i], T. Case [a], A. Cooper [i], O. Cramer [l], K.M. Crowe [a], T. Degener [b], H.P. Dietz [l], N. Djaoshvili [l], S. v. Dombrowski [p], M. Doser [f], W. Dünnweber [l], D. Engelhardt [h], M.A. Faessler [l], P. Giarritta [p], R. Hackmann [c], R.P. Haddock [j], F.H. Heinsius [a], M. Herz [c], N.P. Hessey [l], P. Hidas [d], C. Holtzhaußen [h], D. Jamnik [l,2], H. Kalinowsky [c], B. Kalteyer [c], B. Kämmle [g], P. Kammel [a], T. Kiel [h], J. Kisiel [f,3], E. Klempt [c], H. Koch [b], C. Kolo [l], M. Kunze [b], M. Lakata [a], R. Landua [f], J. Lüdemann [b], H. Matthäy [b], R. McCrady [n], J. Meier [g], C.A. Meyer [n], L. Montanet [f], A. Noble [p,4], R. Ouared [f], F. Ould-Saada [p], K. Peters [b], C.N. Pinder [e], G. Pinter [d], C. Regenfus [l], J. Reißmann [g], S. Resag [c], W. Roethel [l], P. Schmidt [g], I. Scott [i], R. Seibert [g], S. Spanier [p], H. Stöck [b], C. Straßburger [c], U. Strohbusch [g], M. Suffert [o], U. Thoma [c], M. Tischhäuser [h], D. Urner [p], C. Völcker [l], F. Walter [k], D. Walther [b], U. Wiedner [f], B.S. Zou [i],

[a] *University of California, LBNL, Berkeley, CA 94720, USA*

[b] *Universität Bochum, D-44780 Bochum, FRG*

[c] *Universität Bonn, D-53115 Bonn, FRG*

[d] *Academy of Science, H-1525 Budapest, Hungary*

[e] *Rutherford Appleton Laboratory, Chilton, Didcot OX11 0QX, UK*

[f] *CERN, CH-1211 Geneva 4, Switzerland*

[g] *Universität Hamburg, D-22761 Hamburg, FRG*

[h] *Universität Karlsruhe, D-76021 Karlsruhe, FRG*

[i] *Queen Mary and Westfield College, London E1 4NS, UK*

[j] *University of California, Los Angeles, CA 90024, USA*
[k] *Universität Mainz, D-55099 Mainz, FRG*
[l] *Universität München, D-80333 München, FRG*
[m] *LPNHE Paris VI, VII, F-75252 Paris, France*
[n] *Carnegie Mellon University, Pittsburgh, PA 15213, USA*
[o] *Centre de Recherches Nucléaires, F-67037 Strasbourg, France*
[p] *Universität Zürich, CH-8057 Zürich, Switzerland*

A study of p̄-annihilation in liquid deuterium into $\pi^-\pi^0\pi^0$ and a spectator-proton is presented. A cut on the proton-momentum of $\leq$ 100 MeV/c ensures that annihilation takes place on a quasi-free neutron. A partial wave analysis shows contributions from three vector mesons, with masses and widths of $(763.7 \pm 3.2; 152.8 \pm 4.3)$, $(1411 \pm 14; 343 \pm 20)$; $(1780^{+37}_{-29}; 275 \pm 45)$ MeV/c^2, respectively.

The question of the mass of the first radial excitation of the $\rho(770)$ has been a controversial issue since the first claim for its observation in 1971 [1]. The presently accepted mass of the lowest ρ' is at 1450 MeV accompanied by a state at 1700 MeV [2], presumably a $^3D_1$ q̄q-state [3]. The Particle Data Group interprets the early claims for a low–mass ρ' observed in the $\omega\pi$ system [4] in terms of the high–mass tail of ρ decaying into $\omega\pi$. The presently accepted mass assignments are based largely on reanalyses of various data sets by Donnachie and Clegg [5] and on results from the DM2 experiment [6,7]. There are a few points, however, which contradict those findings. From the proton form factor a ρ' mass of 1260 MeV can be inferred [8]. Furthermore, the LASS experiment has recently reported evidence for a narrow low–mass ρ' at (1287±28 MeV) with a width of (87±28 MeV) in an analysis of the channel $\mathrm{K}^-\ p \to \Lambda\ \pi^+\pi^-$[9]. The latter value is in good agreement with the value expected from the mass of the K*(1410) and the ground-state K*(892) $- \rho(770)$ mass splitting. Additionally, in $\bar{p}p$ annihilation at rest, evidence for a ρ radial excitation has been reported [10,11].

---

[1] College of William & Mary, Williamsburg, USA
[2] University of Ljubljana, Ljubljana, Slovenia
[3] University of Silesia, Katowice, Poland
[4] Now at CRPP, Ottawa, Canada

This situation has motivated us to search for vector mesons in the reaction

$$\bar{p}n \rightarrow \pi^-\pi^0\pi^0 \quad (1)$$

by stopping antiprotons in liquid deuterium (LD_2). To ensure that the $\bar{p}$-annihilation occurs on a quasi-free neutron, the proton spectator momentum was limited (by an off-line cut) to a maximum of 100 MeV/c.

The study of $\bar{p}n$ annihilation offers distinct advantages compared to that of $\bar{p}p$ annihilation into $3\pi^0$[12] or into $\pi^+\pi^-\pi^0$[13,11]. Firstly, the $\bar{p}n$-system has isospin I=1; hence annihilation into 3 pions is restricted to the ${}^{2S+1}L_J = {}^1\mathrm{S}_0$, ${}^3\mathrm{P}_1$ and ${}^3\mathrm{P}_2$-states of the $\bar{p}n$-system (these are the same states accessible to $3\pi^0$ in $\bar{p}p$-annihilation). The $\pi^0\pi^0$ interactions are isoscalar (possible isotensor contributions are not considered), and because of G-parity conservation, only S- and D-waves can contribute. Furthermore, in reaction (1) there is only one $\pi^0\pi^0$-combination. The $\pi^-\pi^0$ system, on the other hand, is limited to I = 1, and only odd angular momenta are allowed. At low energies, the $\pi^-\pi^0$ subsystem in reaction (1) must therefore be in a relative P-wave. The absence of P-wave in the $\pi^0\pi^0$-subsystem is a considerable simplification and allows the direct observation of high mass ρ's. This is the great advantage of the $\pi^-\pi^0\pi^0$-final state compared to $\pi^+\pi^-\pi^0$.

The data have been collected with the Crystal Barrel detector at LEAR. This detector is well suited to measure channels with both charged and neutral particles in the final state. This has allowed us to measure for the first time the $\pi^-\pi^0\pi^0(p_{spectator})$-final state, using a liquid deuterium target. The detector has been described in detail elsewhere [14]; only a short summary will be given here.

A 200 MeV/c $\bar{p}$ beam stops in the liquid deuterium target at the center of the detector. The target is surrounded by a pair of cylindrical multiwire proportional chambers (PWC's) and a cylindrical drift-chamber (JDC) with 23 layers. The momentum resolution is $\delta p/p = 6.5\%$ at 1 GeV/c. The JDC is surrounded by a barrel consisting of 1380 CsI(Tl) crystals, pointing towards the target center. The CsI calorimeter covers the polar angles between 12° and 168° with full coverage in azimuth. The useful acceptance for shower detection is $0.95 \times 4\pi$ sr. Typical photon energy resolutions are $\sigma_E/E = 2.5\%$ at 1 GeV, and $\sigma_{\Phi,\Theta} = 1.2°$ in both the polar and azimuthal angles.

The data for the present analysis have been taken with a *one-prong trigger* requiring one hit in the inner PWC and one or two hits in the outer JDC-layers. The following off-line selection criteria were applied :

– Exactly one negative charged track in the JDC
– Exactly 4 photons with energy above 20 MeV

– For each electro-magnetic shower due to a photon, the energy deposit in the central crystal should exceed 10 MeV, to avoid spurious photons due to shower fluctuations (which, for the most part, have low energies)
– No photon should have maximum energy deposit in a crystal adjoining the beam pipe (in order to avoid shower leakage)
– Energy and momentum conservation by constraining the "missing mass" to be consistent with the mass of the spectator proton $p_{spectator}$:
$\mid ((m_{\bar{p}d} \; - \; E_{tot})^2 - \mid \overrightarrow{p_{tot}}^2 \mid - m_p{}^2) \;\; \mid \leq \; 0.5\,\mathrm{GeV}^2\!/c^4$

Data surviving these cuts underwent a kinematic fit to the $\bar{p}d \rightarrow \pi^- 4\gamma \; p_{spectator}$ hypothesis (1C fit) and, in a second step, to all possible 3C-fit hypotheses in which the masses of the two $\gamma\gamma$-pairs were constrained to $\pi^0\pi^0$, $\pi^0\eta$, $\eta\eta$ or $\pi^0\eta'$. Further, we have required $\pi^-\pi^0\pi^0 p_{spectator}$ to be the best hypothesis. The $\pi^-\pi^0\pi^0 p_{spectator}$ final state was separated without feedthrough from misidentified $\gamma\gamma$-pairs. Because of the small number of possible $\gamma\gamma$-combinations per event, the combinatorical background is negligible. Events were rejected if the confidence level was below 10% or $p_{spectator}$ was above $100\,\mathrm{MeV}\!/c$ in momentum. None of the accepted events had a different $\gamma\gamma$-combination with a confidence-level exceeding 10%. The partial wave analysis which follows is not affected by extending the cut on spectator momentum up to $150\,\mathrm{MeV}\!/c^2$. From the 8.01 million triggered events, we have assigned 123,409 events to reaction (1).

A Monte Carlo simulation, based on the CERN program package GEANT, was used to derive detection efficiency. We find that the branching ratio for $\bar{p}d$ annihilations at rest into $\pi^-\pi^0\pi^0$ plus proton is

$$BR(\bar{p}d \rightarrow \pi^-\pi^0\pi^0 \; plus \; proton) = 0.68\% \pm 0.07\% \qquad (2)$$

The branching ratio has been checked against contributions from other decay channels such as $\pi^-\pi^0\eta$ and $\pi^-\pi^0\omega$. Because the calorimeter vetoes additional particles with 98% 4π, the contributions of channels with more than one additional gamma are negligible. The branching ratio itself was determined from 1.86 million events on tape taken with a "minimum bias" trigger requiring an antiproton entering the target but with no constraints on the final state.

The $\pi^-\pi^0\pi^0$ Dalitz plot is presented in Figure 1, the $\pi^-\pi^0$ and $\pi^0\pi^0$ invariant mass distributions in Figure 2. Contamination from other channels, determined using the Monte Carlo simulation, is below 0.5% and distributed smoothly over the Dalitz plot.

The most prominent structures in the Dalitz plot are vertical and horizontal ρ^--bands and a diagonal one arising from the $f_2(1270)$. The f_2 angular

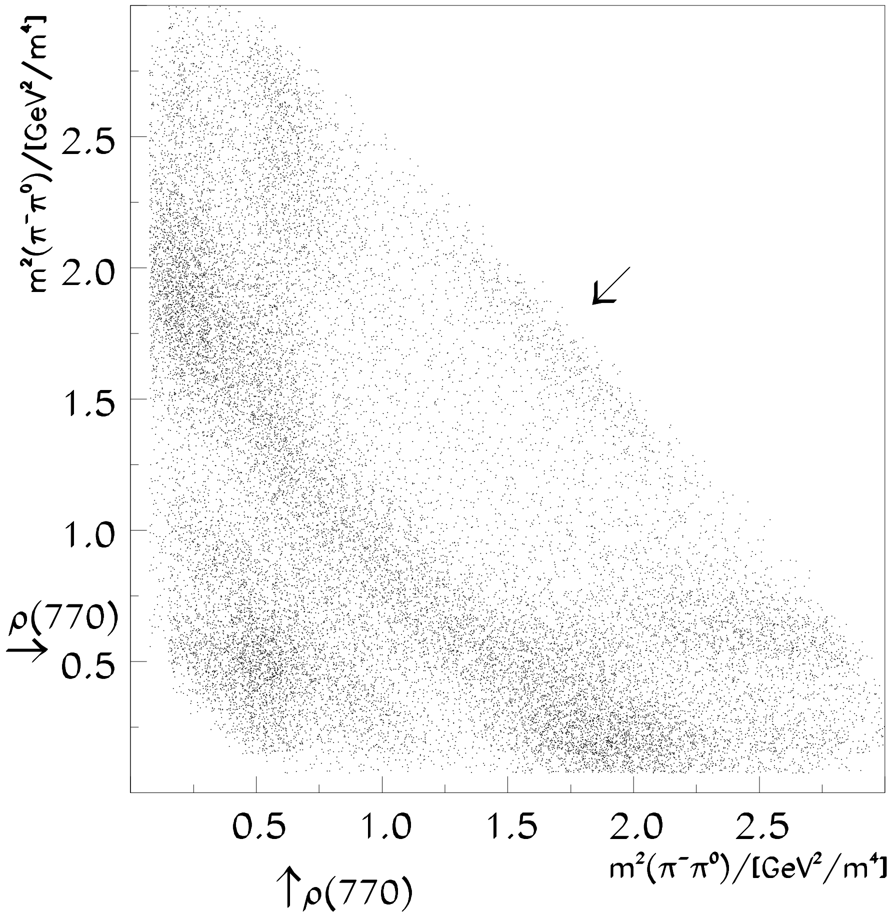

Fig. 1. $\pi^-\pi^0\pi^0$Dalitz-plot ($p_{spectator} \leq$ 100 MeV/c). The diagonal arrow indicates the $\rho^-(1450)$ contribution.

distribution indicates contributions from ^{1}S$_0$ and ^{3}P$_1$ $\bar{p}n$-initial states.

In the lower left corner, a clear band along the second diagonal crossing the two interfering ρ^--bands can be seen. This band can be identified with the $f_0(1500)$. The partial wave analysis shows that an additional tensor contribution in this region improves the fit significantly.

The arrow in Figure 1 marks a contribution which could be associated with the $\pi^0\pi^0$ threshold or with a $\pi^0\pi^-$ resonance at $\sim$1400 MeV/c^2. In the latter case, two $\pi^-\pi^0$ bands interfere in the region indicated by the arrow. A $\pi^0\pi^0$ threshold effect is excluded by the fits. Hence the enhancement is most likely to be interpreted as the interference between two ($\pi^-\pi^0$) P-waves from ^{1}S$_0$ initial state (angular distribution proportional to $cos^2\theta$). In the reaction $\bar{p}p \rightarrow \pi^+\pi^-\pi^0$ this effect is present [10,11] but is masked by the additional

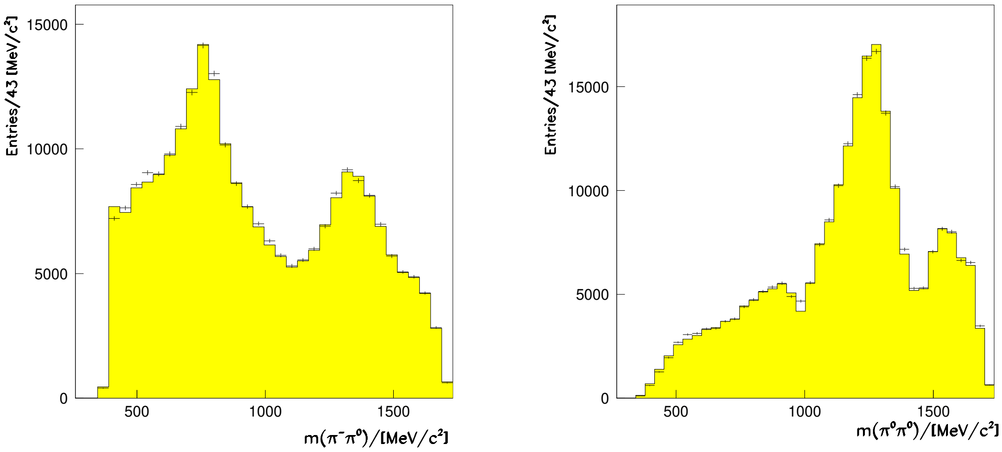

Fig. 2. $\pi^-\pi^0$ and $\pi^0\pi^0$ mass distribution. The data are plotted with error bars and the result of the best fit is overlayed. There are 2 entries per event for the $\pi^-\pi^0$-mass plot.

ρ^0-contribution dominating this part of the Dalitz plot. In the lower right and the upper left corners, small indications of a third $\pi\pi$-P-wave resonance are visible.

The $\pi\pi$ S-, P- and D-wave interactions all contribute to the $\pi^-\pi^0\pi^0$ final state. For the $\pi\pi$ S- and D-wave we imposed a fixed pole-structure from the analysis of $\bar{p}p \rightarrow 3\pi^0$[12], where S- and D-waves can be analysed more easily, because P-wave is absent. The pole structure for S- and D-wave was confirmed by a coupled channel analysis made on the 3 final states : $\bar{p}p \rightarrow 3\pi^0$, $\bar{p}p \rightarrow \eta\pi^0\pi^0$ and $\pi^0\eta\eta$[15]. This S- and D-wave pole structure includes $f_0(980)$, $f_0(400-1200)$, $f_0(1370)$ and $f_0(1500)$ for the S-wave and $f_2(1270)$ and $f_2(1540)/AX$ for the D-wave. In the present analysis, only the production strength and the phases for the S- and D-waves have been varied freely in the fit. The partial wave analysis adopts the isobar model in a P-vector approach. Details of the formalism can be found in [16]. For all contributing partial-waves we used the K-matrix-formalism, thereby ensuring unitary amplitudes for the case of nearby, overlapping resonances. Angular distributions were described by the Zemach formalism [17]. Contributions of the $\pi\pi$ P- and D-wave are allowed from $^1S_0$, $^3P_1$ and $^3P_2$ states, whereas the $\pi\pi$ S-wave is restricted to $^1S_0$ and $^3P_1$ initial states by angular momentum and G-parity conservation.

The $\pi\pi$ P-wave was described by 3 poles with free masses and widths. We find an acceptable description of the data with $\chi^2/N_F = 1305/782$ (825 cells and 43 parameters). A comparison between data and fit in Figure 2 shows that there is no obvious discrepancy. Large χ^2 differences, rather, arise from individual isolated cells contributing more than 4 to the overall χ^2.

The statistical errors on the masses and widths of the $\pi\pi$ P-wave were deter-

Table 1
Masses and widths of $\pi\pi$-P-wave mesons. Given errors are statistical and systematic, respectively.

Meson	Mass (MeV/c^2)	Width (MeV/c^2)
$\rho^-(770)$	$763.7 \pm 3.1_{stat.} \pm 0.5_{syst.}$	$152.8 \pm 4.2_{stat.} \pm 0.8_{syst.}$
$\rho^-(1450)$	$1411 \pm 10_{stat.} \pm 10_{syst.}$	$343 \pm 18_{stat.} \pm 8_{syst.}$
$\rho^-(1700)$	$1780^{+34}_{-25} \pm 14_{syst.}$	$275 \pm 42_{stat.} \pm 17_{syst.}$

mined by a full MINOS-analysis [18]. The systematic errors were determined from a variety of fits with different assumptions as to the production process. The K-matrix formalism adopted here has the disadvantage that the K-matrix-poles are not the physical poles. The latter have been extracted from the fitted amplitudes by an analysis of the different Riemann sheets involved. The masses and widths given in Table 1, having been determined in this way, represent the T-matrix poles.

We now discuss alternative fits. Imposing ρ' and ρ'' parameters as given in [5] results in a small increase in χ^2 by 30 units. Introducing only two P-wave poles leads to a very broad ρ' with $(M;\Gamma) = (1373;537)$ and an increase in χ^2 of 142. The mass and width of this freely fitted ρ' are incompatible with the values given in [2]. Using the parameters for the ρ' as determined by [5], the $\chi 2$ increases by a large amount, $\Delta\chi^2 = +393$. A fit with only one $\rho(770)$ without any higher P-wave-pole contribution yields an unacceptably high χ^2 of 6566. Figure 3 shows the χ^2-distribution of this fit over the Dalitz plot. There are three regions with large χ^2 contributions : the central region is explained in the fit by the interference of two $\rho(1450)$; here data exceed the fit without $\rho(1450)$ and $\rho(1700)$. The same effect and explanation is valid for the small deviations near the edges of the Dalitz plot. The two other regions of large χ^2 differences have fewer entries in the Dalitz plot than required by the fit with only $\rho(770)$. The $\rho(1700)$ leads to destructive interference in this region through its low mass tail. It is this interference, which determines the $\rho(1700)$ pole position.

As mentioned earlier, the LASS collaboration has reported a ρ' at a mass of 1287 MeV/c^2[9]. Imposing the LASS parameters for the ρ' raises χ^2 by 584. In the present work, fits to the data using different starting parameters in all cases converged to the pole structure discussed above. This fact does not exclude the possibility that the $\rho'(1300)$ could be present as an additional resonance. Indeed, a fit with four free $\pi\pi$-P-wave poles improves χ^2 by $\Delta\chi^2$ = -93, but at the expense of the inclusion of eight additional parameters. The resonance pole positions are found at $(763.5 - i77.3), (1321 - i92), (1368 - i128), (1807 - i140)$. However, the additional flexibility of such a fit is likely to be responsible for

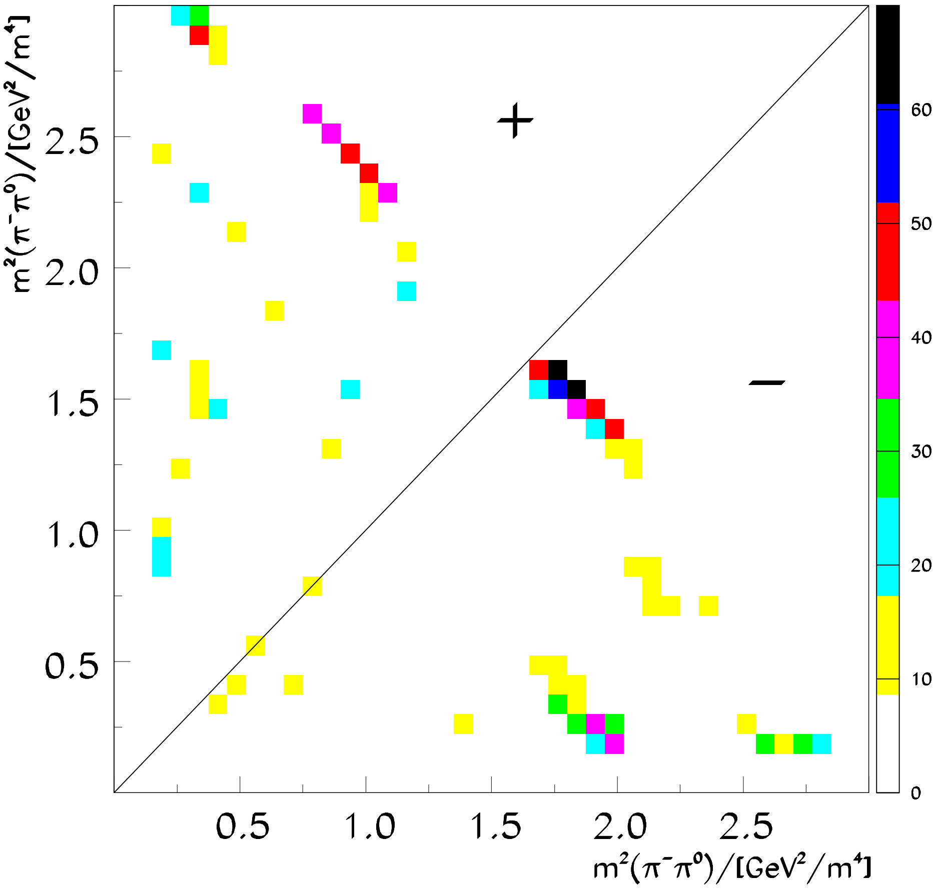

Fig. 3. χ^2-distribution of the fit with only $\rho(770)$ in the $\pi\pi$-P-wave. In the half above the diagonal, the fit exceeds the data (+), whereas in the region marked with (-) data exceeds the fit.

the improvement in χ^2, and we do not claim the observation of four isovector vector resonances.

In [12], two solutions for the $\pi\pi$ S-wave were presented: one with three S-wave poles, the other with four. The fits described so far have used the 4-pole solution. With the 3-pole parametrization for the $\pi\pi$ S-wave we arrive at a slightly improved χ^2 (the same effect having been seen in [12]), but the convergence of the fit is worse, more iterations are needed and the result is characterised by a larger EDM (estimated distance to minimum). The mass of the ρ' is shifted down to 1200 MeV/$c^2$and the width increases to 470 MeV/c^2. The ρ'' remained stable. We consider the four pole solution for the $\pi\pi$ S-wave to give a better description of the data.

Table 2
Branching fractions of the vector mesons after a spectator momentum cut at 100 MeV/c. In the second column the amount of $\pi\pi$-P-wave to the individual initial states is given (normalized to the whole Dalitz plot) and in the fourth column the contribution of each ρ-meson is plotted, summed over the three initial states.

initial state	$\pi\pi$-P-wave	vector meson	contribution
^{1}S$_0$	(13.8±0.9)%	$\rho(770)$	(10.2±2.0)%
^{3}P$_1$	(7.7±0.7)%	$\rho(1450)$	(4.5±0.9)%
^{3}P$_2$	(4.2±0.6)%	$\rho(1700)$	(4.2±0.6)%

The presence of a resonance, referred to as the AX [11], with a mass of 1565 MeV/c^2, a width of 165 MeV/c^2 and strongly produced from P-wave orbitals of the $\bar{p}p$ atom was reported by the Asterix Collaboration and in an analysis of our $3\pi^0$-data [12]. Additional evidence for a structure at this mass had been reported previously [19]. As in [12], exclusion of such a tensor state in the present analysis results in a significantly increased $\Delta\chi^2$ of 205.

The contributions from the various initial states in the best fit are: ^{1}S$_0$: 50%, ^{3}P$_1$: 30% and ^{3}P$_2$: 20%. The errors on the individual branching fractions are about 3%. The branching fractions of the three vector mesons are summed over the 3 possible initial states. The errors were determined from the spread of the individual contributions, determined from several fits, setting individual contributions of the high mass vector mesons from P-wave initial states to zero. The errors for initial state branching fractions were also determined in this way. Table 2 shows the results. The branching fraction of the $f_2(1270)$ after the spectator momentum cut is (19.9±1.2)%, summed over the initial states.

In summary, three ρ-resonances are found necessary to give an acceptable interpretation of reaction (1). The masses and widths determined from a fit, where the pole positions of these resonances are left free, are in good agreement with the values obtained in photo-production (with both virtual and real photons) [5]. The usual interpretation of these resonances are n=1,2 ^{3}S$_1$ and the n=1 ^{3}D$_1$ of the $\pi\pi$-P-wave. Masses and widths agree well with the predictions given in [3]. Close and Page have shown [20], that the 4 π-decay-mode of the $\rho(1450)$ can disentangle the nature of this meson. A study of the 4π decay mode is presently in progress. For the $\pi\pi$-D-wave the data require the existence of a tensor meson above the $f_2(1270)$. This result tends to confirm the previous observations of such a state in $\bar{p}p$ annihilation.

We would like to thank the technical staff of the LEAR machine group and of all the participating institutions for their invaluable contributions to the success of the experiment. We acknowledge financial support from the German

Bundesministerium für Bildung, Wissenschaft, Forschung und Technologie, the Schweizerischer Nationalfonds, the British Particle Physics and Astronomy Research Council, the U.S. Department of Energy and the National Science Research Fund Committee of Hungary (contract No. DE-FG03-87ER40323, DE-AC03-76SF00098, DE-FG02-87ER40315 and OTKA F014357). N. Djaoshvili, F.-H. Heinsius and K.M. Crowe acknowledge support from the A. von Humboldt Foundation.

References

[1] Layssac et al., Nuovo Cim. **6A** (1971) 134.

[2] Particle Data Group (PDG), Phys. Rev. **D50** (1994) 1479.

[3] S. Godfrey, N. Isgur, Phys. Rev. **D 32** (1985) 189.

[4] Frenkiel et al., Nucl. Phys. **B47** (1972) 61.

[5] A.Donnachie and A.Clegg, Z. Phys. **C62** (1994) 455.

[6] Antonelli et al., Phys. Lett. **B212** (1988) 133.

[7] Bisello et al., Phys. Lett. **B220** (1989) 321.

[8] J.G. Körner and M. Kuroda, Phys.Rev. **D16** (1977) 2165.

[9] D. Aston et al., Proc. Hadron 93 conf.,p. 1797, T. Bressani et al. (eds.). Nuovo Cim., **107 A** N.10

[10] Besliu et al., An de fisica **67** (1971) 383.

[11] B. May et al., Z. Phys. **C46** (1990) 203.

[12] Crystal Barrel Collaboration, C. Amsler et al., Phys. Lett. **B342** (1995) 433.

[13] M. Foster et al.,Nucl. Phys. **B6** (1968) 107.

[14] Crystal Barrel Collaboration, E. Aker et al., Nucl. Instrum. Meth. **A 321** (1992) 69.

[15] Crystal Barrel Collaboration, C. Amsler et al., Phys. Lett. **B353** (1995) 571.

[16] S.U.Chung et al., Ann. Phys. **4** (1995) 404.

[17] C. Zemach, Phys. Rev. **B133** (1964) 1201.

[18] F. James et al., MINUIT, CERN-Report CERN-DD D506, CERN, 1987.

[19] L. Gray et al., Phys. Rev. **D27** (1983) 307.

[20] F. Close and P. Page, Nucl. Phys. **B443** (1995) 233.